MEK is a therapeutic and chemopreventative target in squamous cell carcinoma

Adelmann, Charles H.; Truong, Kimberly A.; Liang, Roger J.; Bansal, Varun; Gandee, Leah; Saporito, Rachael

Published in:
Journal of Investigative Dermatology

DOI:
10.1016/j.jid.2016.05.110

Publication date:
2016

Accepted Manuscript

MEK is a therapeutic and chemopreventative target in squamous cell carcinoma

Charles H. Adelmann, Kimberly A. Truong, Roger J. Liang, Varun Bansal, Leah Gandee, Rachael Saporito, Woojin Lee, Lili Du, Courtney Nicholas, Marco Napoli, Barbara Mino, Andrew P. South, Charlotte M. Proby, Irene M. Leigh, Cristian Coarfa, Elsa R. Flores, Kenneth Y. Tsai

PII: S0022-202X(16)31340-9

DOI: 10.1016/j.jid.2016.05.110

Reference: JID 376

To appear in: *The Journal of Investigative Dermatology*

Received Date: 4 January 2016

Revised Date: 18 May 2016

Accepted Date: 19 May 2016

Please cite this article as: Adelmann CH, Truong KA, Liang RJ, Bansal V, Gandee L, Saporito R, Lee W, Du L, Nicholas C, Napoli M, Mino B, South AP, Proby CM, Leigh IM, Coarfa C, Flores ER, Tsai KY, MEK is a therapeutic and chemopreventative target in squamous cell carcinoma, *The Journal of Investigative Dermatology* (2016), doi: 10.1016/j.jid.2016.05.110.

MEK is a therapeutic and chemopreventative target in squamous cell carcinoma

Charles H. Adelmann[1], Kimberly A. Truong[1], Roger J. Liang[1], Varun Bansal[1], Leah Gandee[1], Rachael Saporito[1], Woojin Lee[1], Lili Du[1], Courtney Nicholas[1], Marco Napoli[2], Barbara Mino[1], Andrew P. South[4], Charlotte M. Proby[5], Irene M. Leigh[6], Cristian Coarfa[7], Elsa R. Flores[2], Kenneth Y. Tsai[1,3]

Departments of Translational Molecular Pathology[1], Molecular & Cellular Oncology[2], Dermatology[3]
University of Texas MD Anderson Cancer Center
Houston, TX 77030

Department of Dermatology[4]
Jefferson University
Philadelphia, PA 19107

Centre Molecular Medicine[5]
Jacqui Wood Cancer Centre[6]
University of Dundee
Ninewells Hospital and Medical School
Dundee DD1 9SY
Scotland

Department of Molecular Biology[7]
Baylor College of Medicine
Houston, TX 77030

Correspondence:

Kenneth Y Tsai, MD, PhD
Departments of Dermatology & Translational Molecular Pathology
2130 West Holcombe Blvd, LSP9.4218
University of Texas MD Anderson Cancer Center
Houston, TX 77030
713-563-1943
kytsai@mdanderson.org

Short Title: MEK is a target in squamous cell carcinoma

Cutaneous squamous cell carcinoma (cuSCC) is diagnosed over 700,000 times annually, claiming up to 8,800 lives annually, in the US alone (Karia *et al.*, 2013). No standard targeted therapy exists for cuSCC. Exome sequencing of cuSCC suggest that loss-of-function mutations in major tumor suppressor genes such as *NOTCH1/2*, *TP53*, and *CDKN2A* drive tumor development (Li *et al.*, 2015; Pickering *et al.*, 2014; South *et al.*, 2014; Wang *et al.*, 2011). No activated oncogene is consistently present in cuSCC. EGFR/HER2 inhibitors, the most tested targeted therapy to date, have had limited success, and whether responses correlate with mutation, amplification, or overexpression of *ErbB* family genes is unresolved (Stratigos *et al.*, 2015).

BRAF inhibitors (BRAFi) induce cuSCC formation (Oberholzer *et al.*, 2012; Su *et al.*, 2012) by increasing MEK/ERK signaling in *BRAF* wild-type contexts (Menzies *et al.*, 2013). While other mechanisms contribute (Vin *et al.*, 2013), co-administration of MEK inhibitors (MEKi) with BRAFi dramatically abrogates cuSCC induction (Flaherty *et al.*, 2012). Elevated phospho-MEK/ERK is also seen in sporadic human cuSCC (Dajee *et al.*, 2003; Einspahr *et al.*, 2012). With these rationales in mind, we tested if MEK signaling is necessary for cuSCC induction and maintenance, and whether MEK inhibition is an actionable approach for treatment and chemoprevention of sporadic cuSCC.

To test the effects of MEK inhibition across cuSCC cases with different etiologies and mutational profiles, we tested responses to two MEKi, trametinib and cobimetinib, in 10 lines from both immunocompromised and immunocompetent patients (Vin *et al.*, 2013; Watt *et al.*, 2011). Nine out of ten lines responded to both trametinib and cobimetinib at the highest

concentrations tested (1 μM and 10 μM, respectively), but sensitivity between lines at lower doses was heterogeneous (Figure 1a, Supplementary Figure S1). No clear segregation of sensitive and insensitive lines was revealed, and mutational status of *RAS* or *EGFR* did not correlate with sensitivity (Supplementary Table S1).

To confirm the on-target activity of trametinib and cobimetinib, signal transduction pathway changes in MEK/ERK were probed. Downstream phospho-ERK (pERK) was strongly suppressed at 72 hr by MEKi (Figure 1b), although phosphorylated MEK increased with MEKi treatment. Similar results were obtained with cobimetinib after 72 hr, although the levels of pERK in SRB1 and SRB12, the least sensitive lines tested, were more modestly suppressed with 25 nM treatment (Figure 1c), suggesting incomplete signaling inhibition could explain differences in sensitivity between lines.

We next sought to characterize the cellular response that accompanied the effectiveness of MEK inhibition. In four cuSCC cell lines spanning a range of sensitivities to MEKi, cell cycle progression as measured by EdU nucleotide incorporation was strongly (from 2.5 to 37.9-fold) down-regulated by treatment with both MEK inhibitors (Figure 1d, Supplementary Figure S2), with no significant apoptosis. Consistent with this, we observed a dose-dependent decrease in Cyclin D1 levels following both trametinib and cobimetinib treatment (Figure 1f). No change in Cyclin D1 was detected in SRB12 with either treatment, consistent with this line being the least sensitive in our viability screen (Figure 1a, Supplementary Figure S1). MEK inhibitor treated cuSCC cells became enlarged and flattened (Supplementary Figure S3), a morphological hallmark of senescence (Munoz-Espin and Serrano, 2014). Staining for senescence associated β-

galactosidase (SA-β-gal) activity revealed induction in 9.2 ± 2.0 to 18.6 ± 1.8% of cells in treated populations ($p<0.05$, Figure 1e, Supplementary Figure S3.). Additionally, p21 (*CDKN1A*), a cell-cycle inhibitor and marker of senescence (Munoz-Espin and Serrano, 2014), was induced in all tested lines after trametinib and cobimetinib treatment, except in cobimetinib-treated SRB12 cells, which were relatively resistant (Figure 1g). We also observed that phospho-AKT levels were unchanged only in relatively resistant lines, and that co-targeting AKT resulted in enhanced responses (Supplementary Figure S4).

To test if MEK inhibition could reduce tumor growth *in-vivo*, we established SRB1 tumor xenografts in NOD.Cg-*Prkdc*^{scid} *Il2rg*^{tm1Wjl}/SzJ (NSG) mice and treated with oral trametinib (2mg/kg/day). At sacrifice, average vehicle tumor volume was 3.1-fold larger than trametinib treated tumors ($p<0.0001$, Fig 1h-i). Western-blot analysis of tumor lysates confirmed that trametinib significantly reduced pERK/tERK levels *in-vivo* on an average of 9.8-fold ($p=0.03$, Figure 1j-k), demonstrating successful target engagement in tumors. Together, these data suggest MEK tumor signaling drives proliferation and prevents tumor suppressive senescence induction in cuSCC cells and tumors (Figure 1l), an effect that can be exploited by targeting MEK *in-vivo.*

To better study the effects of MEK inhibition on both cuSCC induction and growth, oral trametinib (2 mg/kg/day) and cobimetinib (10 mg/kg/day) were tested in a UV-driven Hairless mouse model of cuSCC using chronic, low-dose, solar simulated UV light (12.5 kJ/m^2 UVB weekly administered across three doses, Figure 2a), which more faithfully recapitulates human cuSCC molecularly than chemical carcinogenesis models (Vin *et al.*, 2013). Over the course of treatment, control mice formed substantially more tumors than those treated with trametinib or

cobimetinib (Figure 2b). Spaghetti plots of individual lesions and comparisons of lesion sizes at sacrifice confirmed that trametinib completely suppressed detectable net tumor induction, while cobimetinib reduced tumor number versus baseline (Figure 2c-d).

Tracking of individual tumors revealed that trametinib-treated tumors had a 2.4-fold reduced tumor volume increase versus control, while cobimetinib-treated ones showed 5.0-fold growth suppression (Figure 2e). Ki67 staining was reduced by 24% trametinib and 18% for cobimetinib ($p=0.002$, $p=0.02$, Figure 2f-g), and target pathway engagement was confirmed with suppression of ERK activation by up to 39% (Supplementary Figure S5). Overall, 62-69% of papillomas responded and 50-75% of cuSCCs responded to MEKi (Supplementary Figure S6).

Our results suggest that MEK is an effective target for preventing and treating cuSCC. Inhibition of MEK causes senescence, but not apoptosis, of cuSCC cells, with observed synergism with AKT inhibition. The near-complete abrogation of cuSCC induction in our UV-driven model with MEKi indicates that MEK activation is rate limiting for sporadic cuSCC induction, as it appears to be for BRAFi-induced lesions (Flaherty *et al.*, 2012). While responses of existing tumors were heterogeneous, significant suppression of proliferation and phospho-ERK was observed in tumors of treated mice. We conclude that MEK inhibition may be a basis for molecularly targeted chemoprevention and therapy of cuSCC.

CONFLICTS OF INTEREST

There are no relevant conflicts of interest.

ACKNOWLEDGEMENTS

Human cell lines were obtained with written informed patient consent and institutional approval. We thank Pamela A. Villalobos and Jaime Rodriguez Canales (MDACC) for their assistance in the quantitative analysis of IHC (Aperio). Support from the Boone Pickens Endowment for Early Prevention of Cancer (K.Y.T.), NIH 1R01CA194617 (K.Y.T.), Rice Century Scholars (C.H.A.), CPRIT (C.H.A.), Cancer Research UK, European Research Council, and DEBRA-UK (C.M.P., I.M.L., A.P.S.) is acknowledged.

REFERENCES

Dajee M, Lazarov M, Zhang JY, Cai T, Green CL, Russell AJ, *et al.* (2003) NF-kappaB blockade and oncogenic Ras trigger invasive human epidermal neoplasia. *Nature* 421:639-43.

Einspahr JG, Calvert V, Alberts DS, Curiel-Lewandrowski C, Warneke J, Krouse R, *et al.* (2012) Functional protein pathway activation mapping of the progression of normal skin to squamous cell carcinoma. *Cancer Prev Res (Phila)* 5:403-13.

Flaherty KT, Infante JR, Daud A, Gonzalez R, Kefford RF, Sosman J, *et al.* (2012) Combined BRAF and MEK inhibition in melanoma with BRAF V600 mutations. *N Engl J Med* 367:1694-703.

Karia PS, Han J, Schmults CD (2013) Cutaneous squamous cell carcinoma: estimated incidence of disease, nodal metastasis, and deaths from disease in the United States, 2012. *J Am Acad Dermatol* 68:957-66.

Li YY, Hanna GJ, Laga AC, Haddad RI, Lorch JH, Hammerman PS (2015) Genomic analysis of metastatic cutaneous squamous cell carcinoma. *Clin Cancer Res* 21:1447-56.

Menzies AM, Kefford RF, Long GV (2013) Paradoxical oncogenesis: are all BRAF inhibitors equal? *Pigment Cell Melanoma Res* 26:611-5.

Munoz-Espin D, Serrano M (2014) Cellular senescence: from physiology to pathology. *Nat Rev Mol Cell Biol* 15:482-96.

Oberholzer PA, Kee D, Dziunycz P, Sucker A, Kamsukom N, Jones R, *et al.* (2012) RAS mutations are associated with the development of cutaneous squamous cell tumors in patients treated with RAF inhibitors. *J Clin Oncol* 30:316-21.

Pickering CR, Zhou JH, Lee JJ, Drummond JA, Peng SA, Saade RE, *et al.* (2014) Mutational landscape of aggressive cutaneous squamous cell carcinoma. *Clin Cancer Res* 20:6582-92.

South AP, Purdie KJ, Watt SA, Haldenby S, den Breems NY, Dimon M, *et al.* (2014) NOTCH1 mutations occur early during cutaneous squamous cell carcinogenesis. *J Invest Dermatol* 134:2630-8.

Stratigos A, Garbe C, Lebbe C, Malvehy J, del Marmol V, Pehamberger H, *et al.* (2015) Diagnosis and treatment of invasive squamous cell carcinoma of the skin: European consensus-based interdisciplinary guideline. *Eur J Cancer* 51:1989-2007.

Su F, Viros A, Milagre C, Trunzer K, Bollag G, Spleiss O, *et al.* (2012) RAS mutations in cutaneous squamous-cell carcinomas in patients treated with BRAF inhibitors. *N Engl J Med* 366:207-15.

Vin H, Ojeda SS, Ching G, Leung ML, Chitsazzadeh V, Dwyer DW, *et al.* (2013) BRAF inhibitors suppress apoptosis through off-target inhibition of JNK signaling. *Elife* 2:e00969.

Wang NJ, Sanborn Z, Arnett KL, Bayston LJ, Liao W, Proby CM, *et al.* (2011) Loss-of-function mutations in Notch receptors in cutaneous and lung squamous cell carcinoma. *Proc Natl Acad Sci U S A* 108:17761-6.

Watt SA, Pourreyron C, Purdie K, Hogan C, Cole CL, Foster N, *et al.* (2011) Integrative mRNA profiling comparing cultured primary cells with clinical samples reveals PLK1 and C20orf20 as therapeutic targets in cutaneous squamous cell carcinoma. *Oncogene* 30:4666-77.

FIGURE LEGENDS

Figure 1. MEK inhibition prevents cell cycling and induces senescence in human models of cuSCC. (a) Trametinib and cobimetinib viability dose response curves measured by Cell Titer Glo after 72 hr of continuous drug treatment. Half-maximal effect (IC_{50}), maximal effect (E_{max}), and area under the curve (AUC) measurements are graphically represented in Supplementary Figure S1. **(b-c)** MEK/ERK signal transduction western blotting after 72 hr of treatment of MEKi at indicated dose. **(d)** EdU cell cycle staining after 72 hr treatment with trametinib (150 nM) or cobimetinib (250 nM). Cells were labeled with 10 μM EdU for 2.5 hours before fixing, counterstaining, and quantifying with the Nexcelom Celligo System. **(e)** Senescence associated -β-galactosidase senescence staining with X-gal after 72 hr treatment with trametinib (150 nM) or cobimetinib (250 nM). Positive cells were quantified manually. **(f)** Western blot for cell cycle marker Cyclin D1 after 72 hr of MEKi treatment. **(g)** Western blot for senescence marker p21 after 72 hours of MEKi treatment indicated. **(h)** Representative photographs of vehicle and oral trametinib-treated (2mg/kg/day) SRB1 xenograft in NSG mice at sacrifice. **(i)** Tumor volume, tracked by caliper measurement, after treatment initiation. **(j-k)** Quantitation and representative western blot from SRB1 NSG tumor lysates for phospho-ERK engagement. **(l)** Model of MEK involvement in cuSCC tumorigenesis and mechanism of MEKi in preventing cuSCC tumor growth. All error bars are S.E.M. and average at least three independent experiments. *$p<0.05$, **$p<0.01$, †$p<0.001$.

Figure 2. MEK inhibition prevents tumor induction and growth in a spontaneous mouse model of cuSCC. (a) Schematic of experimental design. Full details are in Supplementary Methods. **(b)** Representative image of vehicle, oral trametinib (2mg/kg/day), and oral

cobimetinib (10mg/kg/day)-treated mice before sacrifice. Large lesions (cuSCC) and smaller 'papillomas' are observable on the backs of each mouse. **(c)** Spaghetti plots of changes in tumor number over time. Each line represents one mouse. Matched controls are shown in separate trametinib and cobimetinib plots for clarity. **(d)** End-point quantification of change in tumor number at sacrifice. (Box and whisker plots represent interquartitle range, '+' denotes the mean, Left to right: n = 11,10,10, One-sided t-test against no tumor net induction, i.e. 0). **(e)** End-point quantification of tumor size, measuring fold-change in tumor volume from tumors existing at treatment initiation. Note the y-axis is broken into two segments (Box and whisker plots represent interquartile (IQR) range with outliers excluded by Tukey's criteria, ≥ 1.5 IQR; '+' represents mean values; Left to right: n = 51, 53, 45; t-test compares treatments to vehicle control). **(f)** Ki-67 staining of FFPE fixed lesions at sacrifice. Scale bar (yellow) is 300 µm. **(g)** Automated quantification of Ki-67 positive nuclei processed from whole lesion sections. (Horizontal line is mean; error bars are S.E.M; Left to right: n = 19, 20, 20; t-test compares treatments to vehicle control) *$p<0.05$, **$p<0.01$, †$p<0.001$.

FIGURE 1

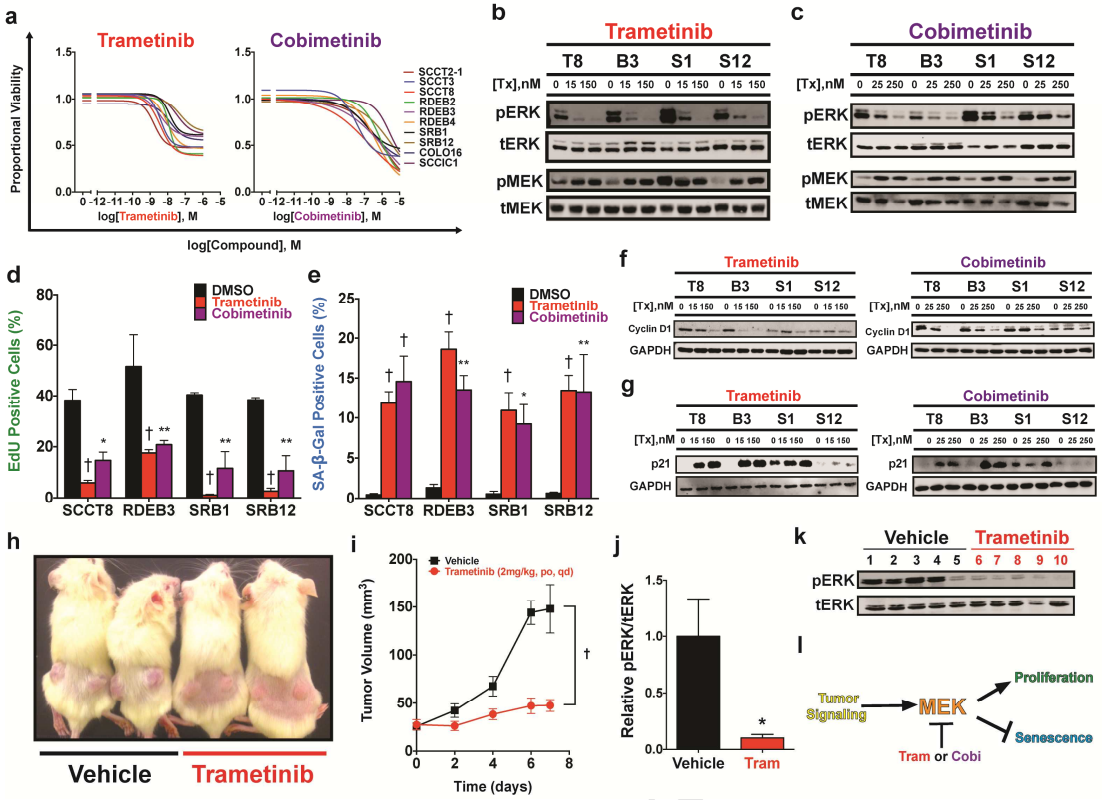
a
Trametinib
Cobimetinib
Proportional Viability
log[Trametinib], M
log[Cobimetinib], M
log[Compound], M
SCCT2-1
SCCT3
SCCT8
RDEB2
RDEB3
RDEB4
SRB1
SRB12
COLO16
SCCIC1
b
Trametinib
T8 B3 S1 S12
[Tx],nM
pERK
tERK
pMEK
tMEK
c
Cobimetinib
d
DMSO
Trametinib
Cobimetinib
EdU Positive Cells (%)
SCCT8 RDEB3 SRB1 SRB12
e
SA-β-Gal Positive Cells (%)
f
Cyclin D1
GAPDH
g
p21
h
Vehicle
Trametinib
i
Vehicle
Trametinib (2mg/kg, po, qd)
Tumor Volume (mm3)
Time (days)
j
Relative pERK/tERK
Vehicle
Tram
k
l
Tumor Signaling
MEK
Proliferation
Senescence
Tram or Cobi

FIGURE 2

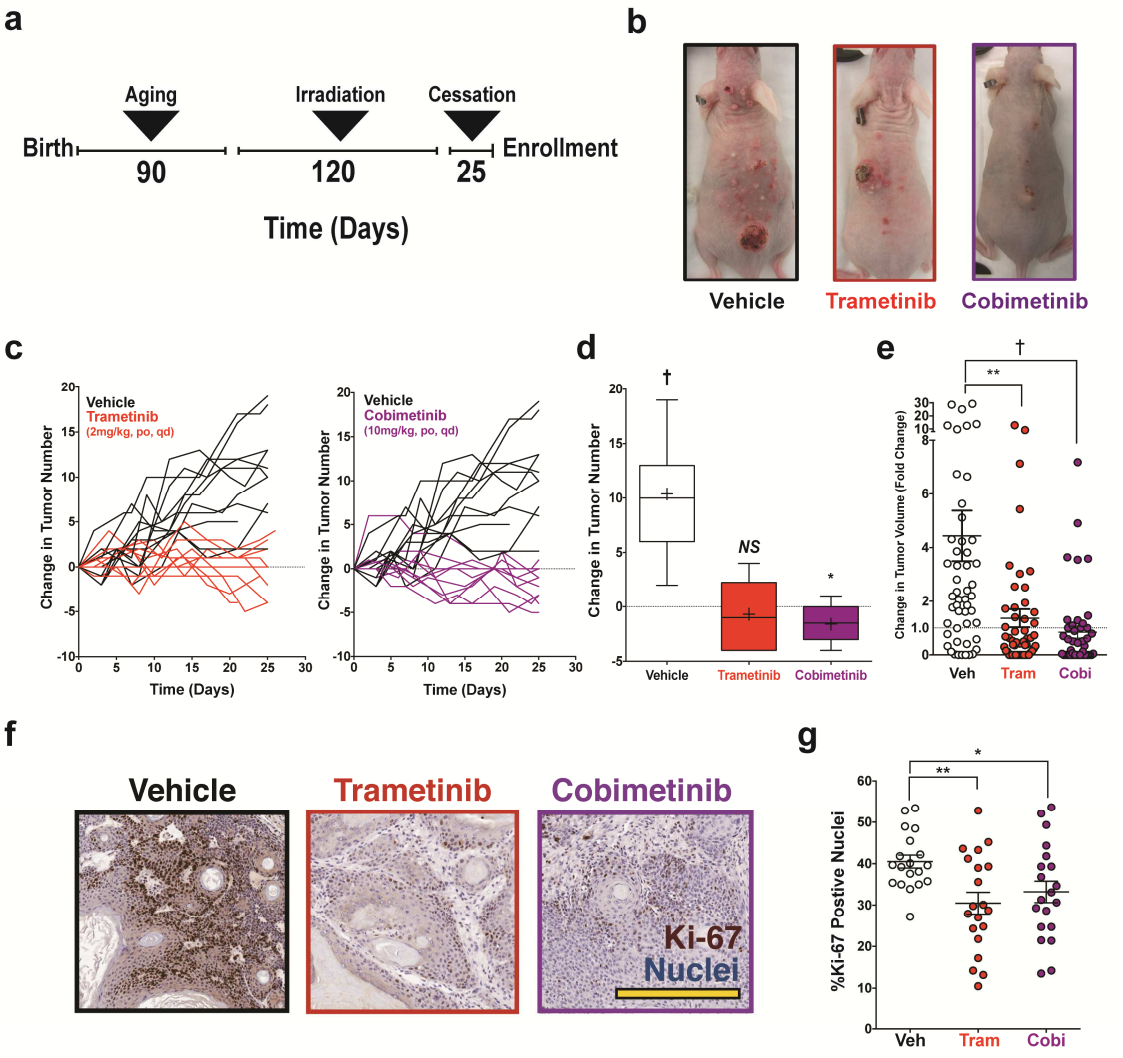
a
Aging
Irradiation
Cessation
Birth
Enrollment
90
120
25
Time (Days)
b
Vehicle
Trametinib
Cobimetinib
c
Vehicle
Trametinib
(2mg/kg, po, qd)
Change in Tumor Number
Time (Days)
Vehicle
Cobimetinib
(10mg/kg, po, qd)
Change in Tumor Number
Time (Days)
d
†
NS
*
Change in Tumor Number
Vehicle
Trametinib
Cobimetinib
e
†
**
Change in Tumor Volume (Fold Change)
Veh
Tram
Cobi
f
Vehicle
Trametinib
Cobimetinib
Ki-67
Nuclei
g
*
**
%Ki-67 Postive Nuclei
Veh
Tram
Cobi